Tone and Broadband Noise Separation from Acoustic Data of a Scale-Model Contra-Rotating Open Rotor

Dave Sree[1]
Tuskegee University, Alabama, USA

David B. Stephens[2]
NASA Glenn Research Center, Ohio, USA

Renewed interest in contra-rotating open rotor technology for aircraft propulsion application has prompted the development of advanced diagnostic tools for better design and improved acoustical performance. In particular, the determination of tonal and broadband components of open rotor acoustic spectra is essential for properly assessing the noise control parameters and also for validating the open rotor noise simulation codes. The technique of phase averaging has been employed to separate the tone and broadband components from a single rotor, but this method does not work for the two-shaft contra-rotating open rotor. A new signal processing technique was recently developed to process the contra-rotating open rotor acoustic data. The technique was first tested using acoustic data taken of a hobby aircraft open rotor propeller, and reported previously. The intent of the present work is to verify and validate the applicability of the new technique to a realistic one-fifth scale open rotor model which has 12 forward and 10 aft contra-rotating blades operating at realistic forward flight Mach numbers and tip speeds. The results and discussions of that study are presented in this paper.

I. Introduction

RECENTLY, there has been a renewed interest in the research and development of contra-rotating open rotor technology for aircraft propulsion application [1]. Studies on open rotors technology have projected that up to 40% reduction in fuel consumption can be achieved compared with presently flying 1990's technology turbofans [2]. This is principally due to the very high propulsive efficiency possible with open rotors when compared to turbofans, but there are practical limitations. Vibration, noise, and structural integrity are some of the problems that pose technological challenges in the practical application of open rotor systems.

The NASA Glenn Research Center (GRC), in collaboration with GE Aviation, has conducted theoretical and experimental studies on open rotor technologies to address some of these problems. Extensive tests have been conducted in low- and high-speed wind tunnels to determine both the far- and near-field acoustic characteristics of a model open rotor. This is a non-proprietary one-fifth scale model blade set, called F31/A31 model, whose aerodynamic and acoustic data can be disseminated [3] [4]. This blade set serves as a baseline design for comparison with other open rotor blade designs (see, for example, reference [5]).

The determination of the tonal and broadband components of noise from these test data is very important for properly assessing the noise control parameters and also for validating the noise prediction codes [6] [7]. The primary technique of *phase averaging* that has been successfully used for processing single rotor (such as turbofan) test data does not work for contra-rotating open rotor acoustic data in the sense that the tonal and broadband noise components cannot be separated properly. This is due to phase shifts that occur in the measured data, as will be explained in Section III. In the past, the broadband noise has been approximated by "chopping off" the "tonal parts" of the total noise spectra at their base and considering the remaining part as the broadband noise [4] [8]. The principal problem with doing this is that it is subjective, requiring a user to specify either an expected tone height (when using a peak-finding algorithm), or a tone width (when using a moving window filter). The results must be checked against the user's expectations. In contrast, phase averaging provides an unambiguous definition for the tones generated by a single shaft fan. There was a need for an analogous data processing tool for open rotors.

[1] Professor, Mechanical Engineering Department, Tuskegee, AL 36088.
[2] Research Aerospace Engineer, Acoustics Branch, Cleveland OH, 44135, AIAA Lifetime Member.

One method that was investigated was the use of the Vold-Kalman order tracking filter, with results published in a recent report [9]. In parallel, a new open rotor signal processing technique was developed by Sree [10] using acoustic measurements of a hobby aircraft contra-rotating propeller having 4 forward and 3 aft blades. The method was reasonably successful in separating tone and broadband noise components. The objective of the present work is to verify and validate the applicability of this technique to data from the open rotor system tested at NASA GRC. Relevant information about the model, its acoustics measurements, and a brief description of the new signal processing technique are given in the sections to follow. Then, the applicability of this technique and its limitations are discussed using representative noise spectra of F31/A31. Finally, conclusions from this study are presented.

II. F31/A31 Open Rotor Model

The F31/A31 model has two contra-rotating rotors. The axial distance between their pitch axes is 19.9 cm (7.8 in). The forward rotor is 65.2 cm (25.7 in) in diameter and has 12 blades whereas the aft rotor is 63.0 cm (24.8 in) in diameter and has 10 blades. The hub diameter of the forward rotor is 26.6 cm (10.5 in) and that of the aft rotor is 24.6 cm (9.7 in). The blades are made of carbon fiber composite with a metal spar. The pitch of the blades can be manually adjusted between tunnel runs to obtain the desired simulated flight condition, i.e., takeoff, approach, or cruise. The F31/A31 model rotors were mounted on a test stand called the Open Rotor Propulsion Rig (ORPR) in a simulated pusher arrangement. The 9- by 15-Foot Low Speed Wind Tunnel (LSWT) (see Figure 1) at GRC was used for the take-off and approach conditions whereas the tests at simulated cruise conditions were conducted in the 8- by 6-Foot Supersonic Wind Tunnel (SWT) (see Figure 2). The ORPR is driven by a pair of uncoupled air turbines fed by high-pressure air at about 20 atm (300 psi) to turn the rotor blades. Additional information on F31/A31 model and test configurations can be obtained from references [3] and [4].

Figure 1. Photograph of the ORPR with F31/A31 blades in the 9x15 LSWT. Traversing microphone shown in foreground. NASA image C-2010-3454.

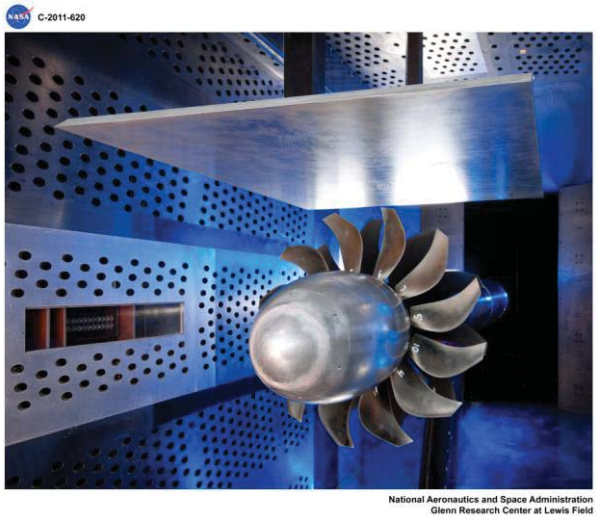

Figure 2. Photograph of the ORPR with F31/A31 blades in the 8x6 SWT. Kulite sensor plate shown above model. NASA image C-2011-620.

III. Acoustic Measurement of F31/A31 Model

All acoustic measurements presented in this reports were performed by running both rotors at the same nominal speed. A feedback controller was used to open and close the air supply valves to vary the speed of each rotor. Far-field sideline acoustic measurements at simulated take-off and approach conditions were made using a traversing microphone probe on a track parallel to and 152.4 cm (60 in) away from the model rotational axis. The microphone and its track can be seen in Figure 1. Data were taken at 18 positions, or stops, as the traverse moved from the rear

side to the front side of the model during each test run. More details about the acoustic instrumentation are provided in [11]. The vast majority of the tests in the low-speed tunnel were performed at a free stream Mach number of 0.2.

Near-field acoustic measurements at simulated cruise conditions in the high-speed tunnel were made using 17 flush-mounted microphones on a plate. The data were collected simultaneously at 17 axial locations above the rotors. The plate could be moved up or down to vary the measurement distance from about 42.6 cm (16.8 inches) to 116.1 cm (45.7 inches) relative to the rotational axis of the rotors. The tests in the high-speed tunnel were performed at various free stream Mach numbers ranging from 0.27 to 0.85. The unsteady pressure data, along with shaft "once-per-revolution" (OPR) signals from both forward and aft rotors, were acquired simultaneously using a sampling frequency of 200 kHz. Each test run had 3 million samples (15 seconds) collected at every measurement location. All spectra shown in Figure 5 through Figure 10 are from the sensors at 90º geometric angle, defined as broadside to the aft rotor.

The acoustic spectra from open rotor systems are known to be dominated by a profusion of tones, although the broadband component is also a significant contributor to the total sound level [8]. The shaft order is defined as, $\mathrm{SO} = f/\Omega$, where f is frequency and Ω is the shaft rotation rate in hertz. The expected dominant tones are calculated as sums of integer multiples of the 12 front and 10 rear blade counts, $\mathrm{SO}(m,n) = 12m + 10n$, when the shaft speeds are equal. Results in the following section will be in terms of frequency presented as shaft order. The *blade rate tones* occur at expected shaft orders when either *m* or *n* is zero. Tones at shaft orders when *m* and *n* are both non-zero are called *interaction tones*. These expected shaft order tones are tabulated in Table 1.

Table 1. Expected Shaft Order Tones for a 12x10 Open Rotor with Equal Rotor Speeds

	$n = 0$	$n = 1$	$n = 2$	$n = 3$	$n = 4$	$n = 5$	$n = 6$
$m = 0$		10	20	30	40	50	60
$m = 1$	12	22	32	42	52	62	72
$m = 2$	24	34	44	54	64	74	84
$m = 3$	36	46	56	66	76	86	96
$m = 4$	48	58	68	78	88	98	108
$m = 5$	60	70	80	90	100	110	120
$m = 6$	72	82	92	102	112	122	132

In practice, the feedback controller was typically able to keep the two rotors at the desired average speed to within 0.5%, but even this small speed difference is enough to allow the phase between the rotors to change considerably. This makes the generated noise "almost periodic" as described by Magliozzi et al. [12] These small revolution-to-revolution differences are known as "jitter."

IV. The New Data Processing Technique

A brief description of the new data processing technique is given here. More details can be obtained from the paper by Sree [10]. The new technique is based on combining cross-correlation and fast-Fourier transform (FFT) operations and is applied to separate the tonal and broadband noise components from measured raw acoustic data of counter-rotating open rotor systems. First, the raw data, called the "overall" signal, at a given measurement location is broken into small uniform time-series segments. The segment size or length selected depends on the frequency resolution desired. (If the segment length in terms of number of measured data samples is NFFT, then the frequency resolution, Δf, is given by $\Delta f = f_s$ / NFFT, where f_s is the sampling frequency. The spectral values obtained through FFT then will be from zero to the Nyquist frequency, f_s /2.) Starting from the beginning of the time record, a pair of consecutive segments is taken and cross-correlation operation is performed to determine the dominant phase shift between them. The second segment is shifted to align the two segments, and adjacent samples are used as needed so both segments are of the specified length. Then a common segment-averaged mean is computed. This mean signal contains the "tonal" component of the overall signal plus half of the "broadband" signal. The mean is then subtracted from the overall signal to obtain the other half of the "broadband" component. Fast Fourier transform (FFT) operations are performed on the "half broadband" component and the process is repeated until all the segment-pairs in the data set are taken into account. A proper averaging is finally performed, the "half broadband" is doubled to obtain the total broadband spectral density and then the tonal portion is quantified by subtracting the broadband from the total.

V. Comparisons with Phase Averaging

Comparisons were required to validate the new method. The typical method of phase averaging is well defined [12], but it was quickly established that phase averaging does not work satisfactorily with the open rotor system due to the drift in rotor phase permitted by the uncoupled counter-rotation turbine drive system. Examples from attempts to apply phase averaging to the dual rotor system are provided in [9]. Instead, phase averaging and Sree's method [10] were both applied to a typical sample of the single-shaft fan data acquired in the 9x15 LSWT [13]. A visual inspection of the results of the two methods can be made by examining Figure 3 and Figure 4. For both methods, the sum of the "tone" and "broadband" spectra give the total spectrum, so only the separated components are shown. Qualitatively the two methods return very similar results when applied to single-rotation fan measurements. The broadband spectra are very similar, with a few small "tones" visibly remaining in the results from Sree's method, seen at around 3 kHz and 6 kHz in Figure 4. Other results presented later in the paper exhibit a similar behavior and this will be discussed at that time. Quantitatively, the pressure spectral densities from each method could be integrated to get an overall sound pressure level (OASPL). Tone OASPL levels from phase averaging were found to be 92.8 dB from the spectra under consideration compared with 92.6 from the method proposed by Sree while the broadband level was 95.1 dB from phase averaging compared with 95.2 from Sree's method. These results emphasize that for single rotation fans, both methods separate tones and broadband similarly. With respect to differences in the methods, phase averaging reconstructs an entire time series resampled to be equal in rotor phase while Sree's method can be thought of as a variation on standard spectral density estimation methods. In each case the tone and broadband components of the signal arithmetically add to give the total component.

Compared with spectral tone removal techniques (i.e., "mowing the grass") both of these methods can quantify tone levels that are below that of the broadband. Spectral tone methods are also somewhat subjective, requiring parameters for either tone-detection or a moving window filter.

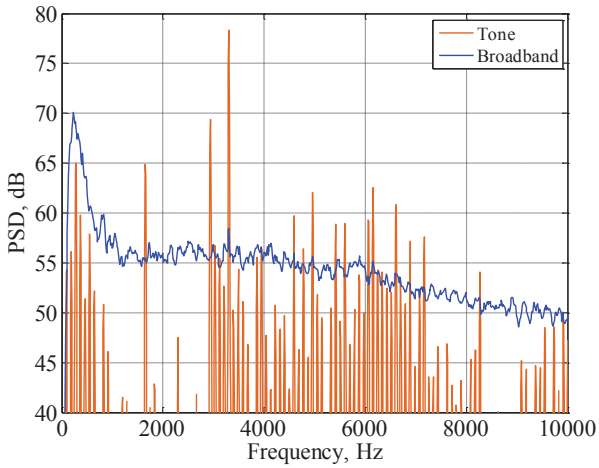

Figure 3. Phase Averaging Tone and Broadband

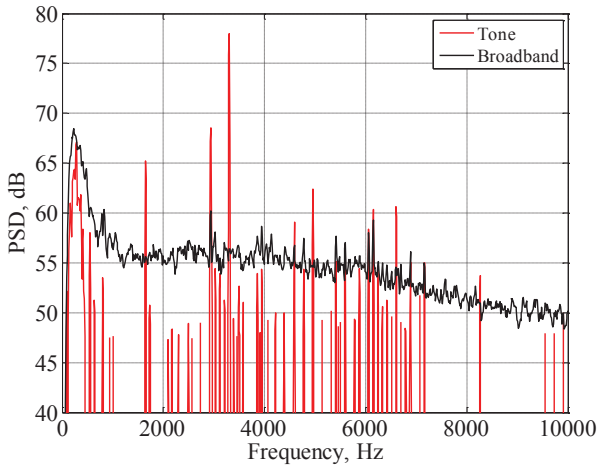

Figure 4. Sree's Method Tone and Broadband

VI. Examples of F31/A31 Noise Spectra and Discussions

Examples to verify the applicability of the new data processing technique for separating tone and broadband noise components are taken from the F31/A31 model test data. The data were acquired with the model positioned at zero angle of attack with no pylon installed. The examples include noise spectra from simulated takeoff, approach, and cruise conditions. Before applying the new technique, the data were preprocessed using a 500 Hz-50 kHz band-pass filter to avoid interference of wind tunnel background noise, particularly at low rotor speeds. Some of the low frequency noise was the empty tunnel background noise while other portions of it are due to the wake from the rotors flowing over the ORPR strut. [15] Methods for accounting for the background noise of the facility have not been included in the tone/broadband results presented in this report. The spectra were computed using a sample size of 3 million and a Fourier transform of length 2^{14} for a frequency resolution of 12.2 Hz. This results in 90 pairs of segments when processing with the new method. The specific results presented in the present report are a small

fraction of the total data volume acquired on this rotor blade set. A table of the reading numbers and a few relevant parameters are shown in Table 2.

Table 2. Selected performance information for measurements used in this report.

Program	Reading Number	Forward Rotor Pitch Angle (degrees)	Aft Rotor Pitch Angle (degrees)	Forward RPM	Aft RPM	Tunnel Mach Number	Forward Rotor Thrust (lbf)	Aft Rotor Thrust (lbf)	Forward Rotor Torque (ft-lbf)	Aft Rotor Torque (ft-lbf)
D074	424	33.5	35.7	6473.0	6473.5	0.20	164.9	152.2	78.8	75.4
D074	430	33.5	35.7	7668.4	7668.3	0.20	299.5	264.3	138.9	125.0
D074	470	40.1	40.8	6486.9	6487.4	0.20	288.0	289.9	167.4	161.2
D106	2948	64.4	61.8	6335.9	6337.2	0.78	213.8	219.7	283.9	253.8
D106	2966	64.4	61.8	6943.2	6943.0	0.78	356.8	443.5	450.8	473.0

A. Noise Spectra at Nominal Take-Off Condition

The computed tonal and broadband noise spectra for the simulated take-off pitch angles (Program D074, Reading 470) are shown in Figure 5 up to SO = 300, corresponding to approximately 32.4 kHz. The same data is plotted only up to SO=80 (8.65 kHz) in Figure 6 and subsequent charts, as the bulk of the tones are below this frequency. The tonal spectrum is shown in red and broadband spectrum in black.

It is seen that the tonal and the broadband noise components are clearly resolved by the new technique. The rotor alone and the rotor-to-rotor interaction tones (multiple harmonics) of the shaft orders 10 (aft rotor) and 12 (forward rotor) can also be observed in these plots. The broadband component shows small "blips," including those at shaft orders 34 and 42, but they are at least two orders of magnitude lower than the corresponding tonal components and are essentially similar to those found in the single rotation fan example (Figure 4). The appearance of these blips may be due to the limitations of the new technique not being able to completely account for all the random phase shifts that occur between the successive data segments. Or, it may be that the wake flow from front rotor is locked on to the aft rotor causing the broadband to become modulated. It is also possible that there may be a strong coupling between tone and broadband noise, which may not be easy to separate. Limitations of the method are investigated in Section VII.

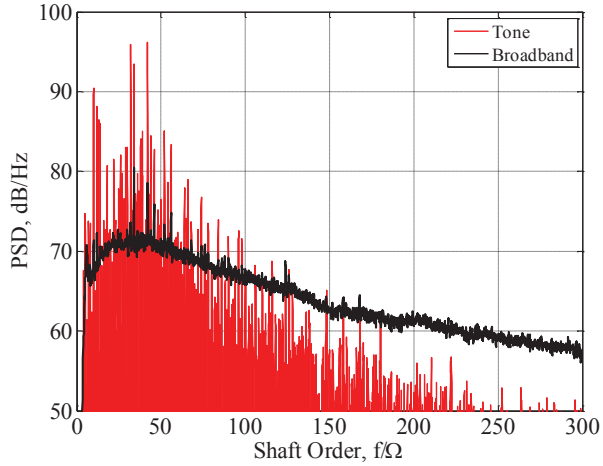

Figure 5. Tonal and broadband spectra at 97% rotor design speed, takeoff pitch angles, Reading 470.

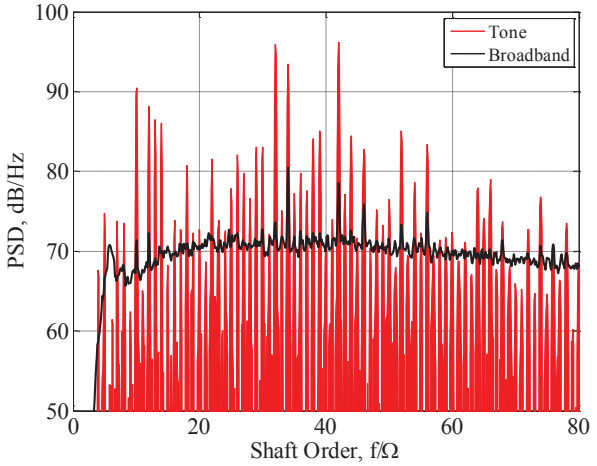

Figure 6. Tonal and broadband spectra at 97% rotor design speed, takeoff pitch angles, Reading 470. Same data as Figure 5.

B. Noise Spectra at Simulated Approach Condition

The processed tonal and broadband spectra for the model at simulated approach condition (Reading 424 of Program D074) are shown in Figure 7. This was chosen because it was run at the same rotor speed as shown for take-off, but is at considerably lower rotor thrust. It is seen that the tonal and the broadband components are separated reasonably well except that the broadband noise shows some small blips, with the biggest offenders being SO = 34, 46, 52, 56 and 68. These tones are not necessarily the largest in the spectrum and referring to Table 1, it is difficult to identify any pattern that would help explain the irregular success of the separation. The main tones in the approach sound spectrum are the rotor blade rate tones (SO = 10, 12), while the take-off spectrum presented above shows many more strong interaction tones. Additionally, the approach broadband spectrum has a number of "haystacks" around SO = 12 + 10*n* (i.e., 12, 22, 32, etc.). These may correspond to an unsteady phenomena, such as the front rotor tip vortex impinging on the aft rotor in a way that is nearly periodic.

Figure 8 shows measurements taken during Reading 430 from the same run as Reading 424 but a few minutes later. The rotor is at a higher operating speed but other conditions were the same. The tone/broadband separation is clearly less than ideal in this case (especially compared with Reading 424 shown in Figure 7), with some tones not at all captured in the appropriate spectrum. This appears to show a weakness in the method, and will be discussed in Section VII.

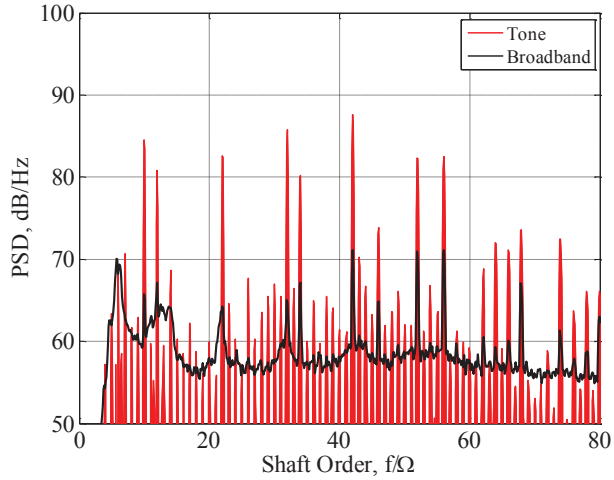

Figure 7. Tonal and broadband spectra 97% rotor design speed, approach pitch angles, Reading 424.

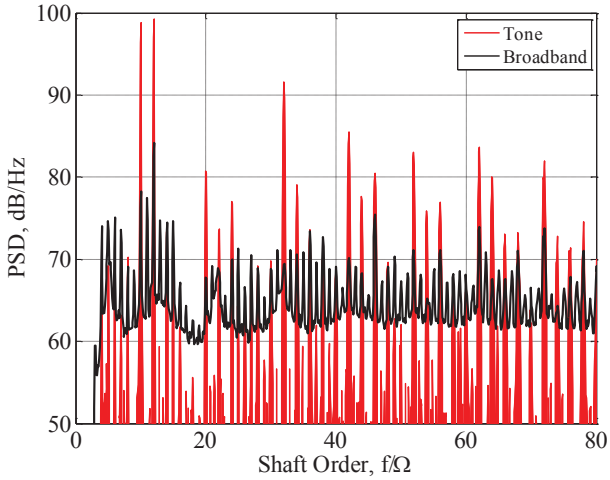

Figure 8. Tonal and broadband spectra 114% rotor design speed, approach pitch angles, Reading 430.

C. Noise Spectra at Simulated Cruise Condition

This example is taken from test data measured at simulated cruise condition in the high-speed wind tunnel with a sensor directly above and 50.8 cm (20 inches) away from the model centerline axis while the rotors were running at 83% design speed (Program D106, Reading 2948). The freestream Mach number was 0.78. The model blade-pitch angles were set at $64.4^{o}/61.8^{o}$. The computed overall noise spectrum and the corresponding tonal and broadband spectra for this case are shown in Figure 9. Here again, it is seen that the tonal and the broadband components are nicely separated. Small blips in broadband noise do appear, but they are well below their corresponding tone levels. The multiple harmonics of the aft rotor shaft order (10) can be clearly seen in these plots. In this particular case, the forward rotor harmonics are lower than the aft rotor ones because of closer proximity (0.81 rotor diameters) of the sensor to the aft rotor. Results from the next higher rotor speed are shown in Figure 10. In a very similar manner to the results for the approach condition, the higher rotor speed noise separation is not as good, even though all other operating conditions are kept the same.

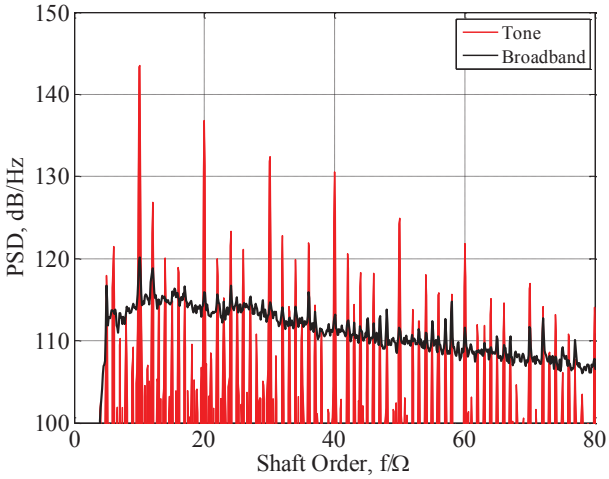

Figure 9. Tonal and broadband spectra, 6336 RPM, cruise pitch angles, Reading 2948.

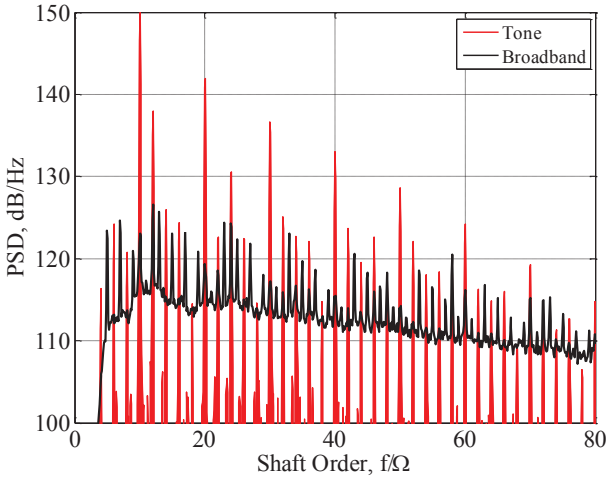

Figure 10. Tonal and broadband spectra, 6943 RPM, cruise pitch angles, Reading 2966.

D. Tone and Broadband Directivity

With the new tool available, it was of interest to investigate the relative contribution of the tones and broadband to the total sound spectra. The three results shown below are for the three readings already presented, where the separation method works well. The spectral results were checked, and good separation was achieved for each of the directivity angles, even though the low Mach number measurements were not acquired simultaneously. The directivity results were computed by integrating the respective pressure spectral density curves between 500 Hz and 50 kHz. Figure 11 shows take-off pitch angles where the broadband is a significant contributor to the total sound pressure level, especially at forward angles. Analogous results are shown for approach pitch angles in Figure 12. The rotor speeds are essentially the same between these two figures, but the more closed pitch angles of the approach setting produce a tone-dominated directivity. Also, the total levels are much lower for Reading 424, as are the thrust and torque.

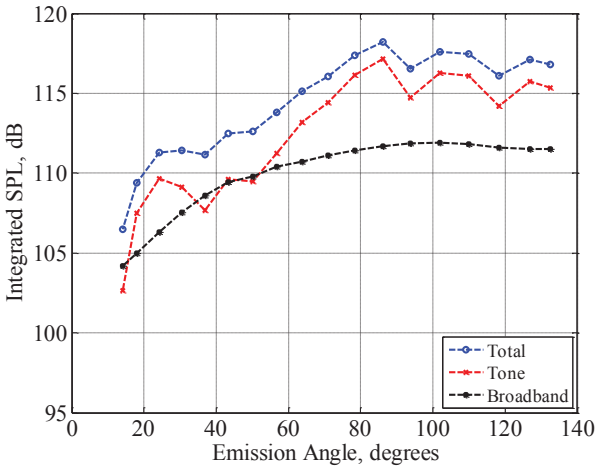

Figure 11. Directivity of tones and broadband at take-off pitch angles. Reading 470.

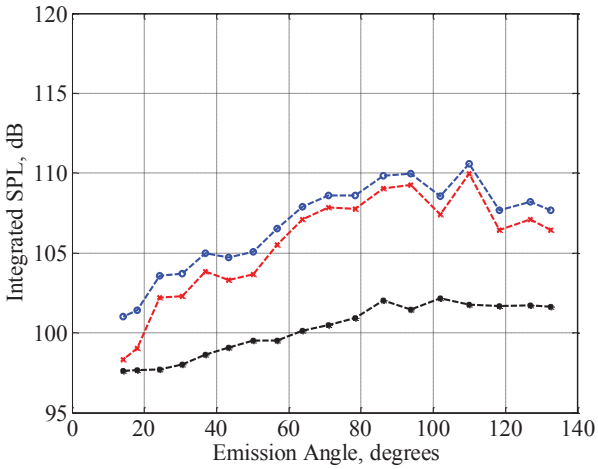

Figure 12. Directivity of tones and broadband at approach pitch angles. Reading 424.

At cruise, the directivity is completely dominated by the forward and aft blade rate tones, which are noticeable as two peaks in Figure 13, with the 90º location sensor directly above the aft rotor. The geometric angle has been used for this chart, since the close sensor location and large unsteady pressure amplitudes casts doubt on the use of linear

acoustic methods. Note that the broadband levels measured by this method may be dominated by aerodynamic pressures on the flush-mounted sensors.

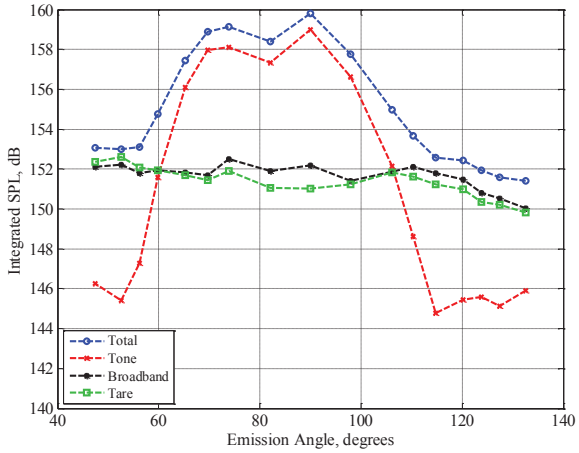

Figure 13. Directivity of tones and broadband for cruise pitch angles. Reading 2948.

VII. Investigation of Limitations

It is shown via the above examples that the new technique has worked reasonably well in separating the tone and broadband noise components from measured raw acoustic data of an open rotor system. However, there were situations encountered during this study where it did not perform well (**Figure 8** and Figure 10), particularly with data at higher rotor speeds. Efforts were made to investigate these results.

The tip relative Mach numbers were calculated to determine if additional noise sources due to rotating shocks were present. For Reading 2948, the tip Mach numbers for the forward and aft rotors were 1.00 and 0.99, respectively, compared with 1.04 and 1.02 for Reading 2966. For the low speed tunnel readings, however, the tip was solidly subsonic, with Mach numbers only up to 0.78 at the fastest tip speeds.

An obvious feature and potential limitation of the method is that is accounts only for the dominant phase shift between the two consecutive segments of the method. It was initially suspected that jitter in the rotors was causing the problem. Since the two shafts are uncoupled, there was significant reliance on the software feedback controller that was reading the rotor speeds and adjusting the air supply valves to keep each rotor at the specified speed. The instantaneous speeds of each rotor are shown in Figure 14 from Reading 430, stop 8. It can be seen that the rotors only deviate from the specified speed by about 0.4 Hz, or 24 RPM, corresponding to 0.3% of the target speed. A more detailed metric came from converting the rotor once-per-revolution signals into phasors, and taking a difference to give the rotor phase drift in radians, shown in Figure 15. The drift is seen to be modest, and with the spectral calculation done using 90 windows, the maximum drift across any window was seen to be about 1/22 of a rotation. These metrics were not found to be meaningfully worse for Reading 430 than for Reading 424, so it was concluded that rotor unsteadiness was not the problem.

Another possibility was the presence of multiple frequencies that might not be aligned with a single phase shift. This would manifest itself as a second peak in the cross-correlation with a different period than the main peak. For Reading 430, a second peak was found as shown in Figure 16**Error! Reference source not found.**. The second peak, however, has the same period as the main peak. Also, Reading 2966 does not show this feature so this possibility was also discarded.

Another limitation is that because the cross correlation method is limited to discrete samples, the phase shifting is restricted to multiples of the data acquisition sample period. The implication of this was tested with simulated data and a compelling result was found. A simple illustration is shown in Figure 17. “Signal 1” was a 1000 Hz tone while “Signal 2” was a 1001 Hz tone, each sampled at 200 kHz. Both were fed into the separation algorithm. The tone levels are essentially identical, indicating that the separation algorithm works, but while the “Signal 1 Broadband” is effectively zero, “Signal 2 Broadband” shows some remaining tone energy at the tone frequency. This remaining energy is more than 40 dB below the original peak, showing most of the tone energy is properly bookkept. This simulated example appears to show the same trend as the experimental data, but admittedly the shaft rates and blade rates in the experiment are not rational fractions of the sample rate. The investigation is ongoing.

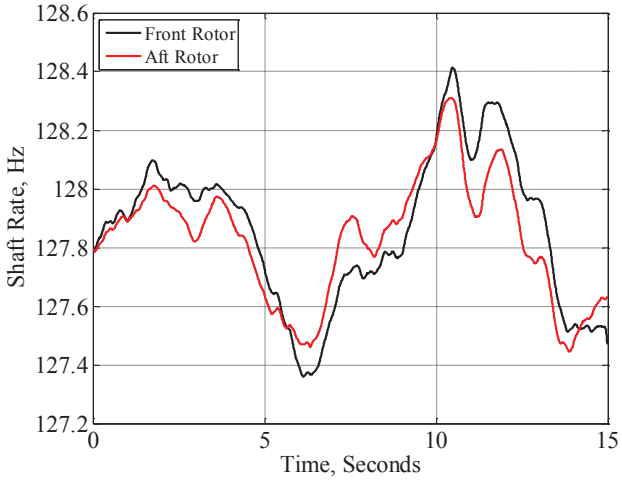

Figure 14. RPM history of front and rear rotors, Reading 430.

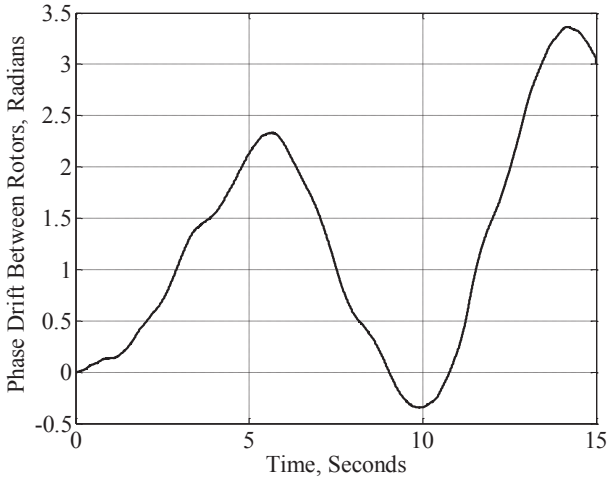

Figure 15. Forward minus aft rotor phase difference angle, Reading 430.

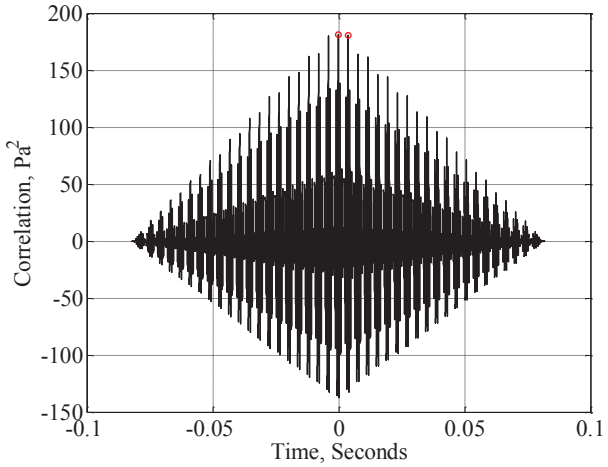

Figure 16. Sample cross-correlation for Reading 430.

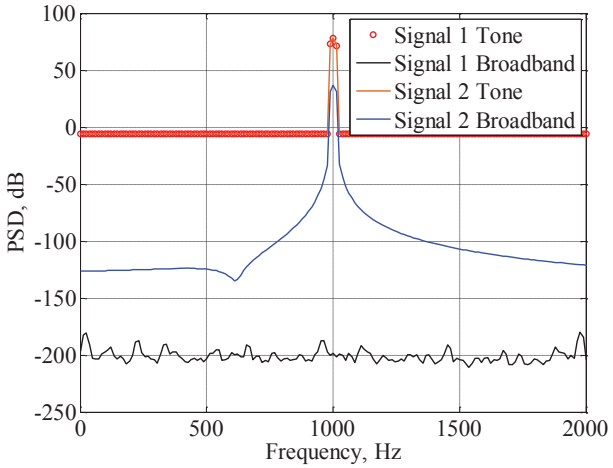

Figure 17. Simulated data example. Note that both "Tone" curves are essentially the same.

VIII. Conclusions

Special signal processing tools are required to characterize open rotor acoustics, particularly the tone and broadband noise characteristics which are important for properly assessing noise control parameters and also for validating open rotor noise prediction codes. A newly published signal processing technique has been applied to separate the tonal and broadband components from measured far- and near-field acoustic data of a one-fifth scale open rotor system having 12 forward and 10 aft blades. A few examples from this open rotor model data have been used to validate applicability of the technique. The study shows that the new technique works reasonably well. However, caution should be exercised in certain cases where the technique does not perform very well due to more dominant and random phase shifts occurring in the measured data. There are now four options for separation tones and broadband. A comparison is provided as Table 3.

Table 3. Comparison of Tone/Broadband Processing Method

	Spectral Methods	Phase Averaging	Order Tracking	Sree's Method
Application	Any	Single shaft	Multi-Shaft	Any
Input	Frequency Spectrum	Time Series	Time Series	Time Series
Output	Frequency Spectra	Time Series	Time Series	Frequency Spectra
Encoder Required	No	Yes	Yes	No
Processing Speed	Fastest	Medium	Slowest	Fast
Other Advantages	Robust	Well defined	Quantifies tone coherence with each shaft	Parameter free
Other Disadvantages	Ad-hoc, subjective		May require filter bandwidth tuning	Only accounts for dominant frequency and harmonics

Acknowledgements

The data processing and analysis presented in this work was performed by Dave Sree under the 2013 Summer NASA-GRC Faculty Fellowship Program and by David B. Stephens who was supported by the Fixed Wing Project of the NASA Fundamental Aeronautics Program. The open rotor experiment was conducted under the NASA Environmentally Responsible Aviation Project of the Integrated Systems Research Program in collaboration with GE Aviation.

References

[1] T. Woods, "Building a Better Plane," 3 May 2010. [Online]. Available: http://www.nasa.gov/topics/aeronautics/features/openrotor_prt.htm. [Accessed 24 April 2014].

[2] M. D. Guynn, J. J. Berton, E. S. Hendricks, M. T. Tong, W. J. Haller and D. R. Thurman, "Initial Assessment of Open Rotor Propulsion Applied to an Advanced Single-Aisle Aircraft (AIAA 2011-7058)," in *11th AIAA Aviation Technology, Integration, and Operations (ATIO) Conference*, Virginia Beach, VA, USA, 20 - 22 September, 2011.

[3] D. M. Elliott, "Initial Investigation of the Acoustics of a Counter Rotating Open Rotor Model With Historical Baseline Blades in a Low Speed Wind Tunnel," in *17th AIAA/CEAS Aeroacoustics Conference*, Portland, OR, 5-8 June, 2011.

[4] D. B. Stephens, "Nearfield Unsteady Pressures at Cruise Mach Numbers for a Model Scale Counter-Rotation Open Rotor," in *18th AIAA/CEAS Aeroacoustics Conference*, Colorado Springs, CO, 4-6 June, 2012.

[5] S. A. Khalid, J. P. Wojno, A. Breeze-Stringfellow, D. P. Lurie, T. H. Wood, K. Ramakrishnan and U. Paliath, "Open Rotor Designs for Low Noise and High Efficiency, GT2013-94736," in *Proceedings*, San Antonio, Texas, USA, June 3-7, 2013.

[6] B. Magliozzi and D. B. Hanson, Propeller and Propfan Noise, Chaper 1, Aeroacoustics of Flight Vehicles: Theory and Practice, Volume 1: Noise Sources, NASA-RP 1258, August 1991.

[7] V. P. Blandeau and P. F. Joseph, "Broadband Noise Due to Rotor-Wake/Rotor Interaction in Contra-Rotating Open Rotors," *AIAA Journal*, vol. 48, no. 11, pp. 2674-2686, 2010.

[8] A. B. Parry, M. Kingan and B. J. Tester, "Relative importance of open rotor tone and broadband noise sources," in *17th AIAA/CEAS Aeroacoustics Conference*, Portland, OR, 5-8 June, 2011.

[9] D. B. Stephens and H. Vold, "Order tracking signal processing for open rotor acoustics," *Journal of Sound and Vibration*, p. In Press, Available Online 21 April, 2014.

[10] D. Sree, "A novel signal processing technique for separating tonal and broadband noise components from counter-rotating open-rotor acoustic data," *International Journal of Aeroacoustics*, vol. 12, no. 1+2, pp. 169-188, 2013.

[11] D. B. Stephens and E. Envia, "Acoustic Shielding for a Model Scale Counter-rotation Open Rotor (AIAA 2011-2940)," in *17th AIAA/CEAS Aeroacoustics Conference*, Portland, Oregon, USA, 05 - 08 June 2011.

[12] B. Magliozzi, D. B. Hanson and R. K. Amiet, "Propeller and Propfan Noise," in *Aeroacoustics of Flight Vehicles: Theory and Practice (NASA TR 90-3052)*, August 1991, pp. 2-64.

[13] J. R. Blough, "A survey of DSP methods for rotating machinery analysis, what is needed, what is available," *Journal of Sound and Vibration*, vol. 262, pp. 707-720, 2003.

[14] E. B. Fite, R. P. Woodward and G. G. Podboy, "Effect of Trailing Edge Flow Injection on Fan Noise and Aerodynamic Performance," in *3rd AIAA Flow Control Conference*, San Francisco, California, USA, 5-8 June 2006.

[15] R. P. Woodward, D. G. Hall, G. G. Podboy and R. J. Jeracki, "Takeoff/Approach Noise for a Model Counterrotation Propeller with a Forward-Swept Upstream Rotor," in *31st AIAA Aerospace Sciences Meeting and Exhibit*, Reno, NV, 1993.